Research Paper

MULTIPLE SCLEROSIS JOURNAL | MSJ

Multiple Sclerosis Journal
18(4) 433–441

DOI: 10.1177/1352458511428464
msj.sagepub.com
SAGE

Quantitative high-field imaging of sub-cortical gray matter in multiple sclerosis

R Marc Lebel[1], Amir Eissa[1], Peter Seres[1], Gregg Blevins[2] and Alan H Wilman[1]

Abstract

Background: In addition to neuronal injury, inflammatory, and demyelinating processes, evidence suggests multiple sclerosis (MS) is also associated with increased iron deposition in the basal ganglia. Magnetic resonance imaging (MRI), particularly at very high field strengths, is sensitive to iron accumulation and may enable visualization and quantification of iron associated with MS.

Objectives: To investigate the sub-cortical gray matter in patients with early-stage relapsing–remitting MS using multiple, and novel, quantitative MRI measures at very high field.

Methods: In total, 22 patients with relapsing–remitting MS and 22 control subjects were imaged at 4.7 Tesla. Transverse relaxation rates (R_2 and R_2^*) and susceptibility phase were quantified in four basal ganglia nuclei, the thalamus, and the red nuclei. Parameters in patients with MS were compared with those in healthy subjects and correlated with clinical scores.

Results: Significant abnormalities were observed in most structures, most notably in the pulvinar sub-nucleus. Significant correlations with disability were observed in the pulvinar; marginally significant correlations were also observed in the thalamus and red nucleus. No significant correlations were observed with duration since index relapse.

Conclusions: Widespread abnormalities are present in the deep gray matter nuclei of patients recently diagnosed with MS; these abnormalities can be detected via multi-modal high-field MRI. Imaging metrics, particularly R_2^*, relate to disease severity in the pulvinar and other gray matter regions.

Keywords

basal ganglia, brain iron, magnetic resonance imaging, multiple sclerosis, susceptibility imaging, transverse relaxometry

Date received: 25th July 2011; revised: 3rd October 2011; accepted: 10th October 2011

Introduction

In addition to inflammation, neuronal injury, and demyelinating processes, increased tissue iron has been observed in patients with multiple sclerosis (MS). Histological studies report abnormal iron levels in neurons and gray matter near lesions,[1] in macrophages and microglia,[2] and in the putamen and thalamus.[3] Magnetic resonance imaging (MRI) corroborates these findings: hypointensity on T_2-weighted images has been observed in most deep gray matter nuclei,[3-6] and quantitative MRI measures strongly suggest increased iron in the basal ganglia.[7] Interestingly, imaging metrics in deep gray matter correlate better with disability[6,8] and cognitive function[9,10] than does T_2 lesion load,[11] the commonly used imaging metric for disease burden.

Iron is a crucial element in the electron transport chain and plays a role in DNA synthesis; however, it must be carefully regulated via chelation to prevent unwanted reactions.[12,13] With inadequate chelation or storage, redox active iron catalytically mediates the production of highly reactive hydroxyl radicals,[14] which are known to denature proteins, damage DNA, and oxidize lipid membranes.[13]

There is between 3–5 g of iron in the human body, approximately two-thirds of which is bound to hemoglobin;[15] 60 mg is distributed throughout the

[1]Department of Biomedical Engineering, Faculty of Medicine and Dentistry, University of Alberta, Canada.
[2]Division of Neurology, Faculty of Medicine and Dentistry, University of Alberta, Canada.

Corresponding author:
R Marc Lebel, Room 1098, Research Transition Facility, University of Alberta, Edmonton, Alberta, T6G 2V2, Canada.
Email: mlebel@gmail.com

brain parenchyma,[16] stored primarily as ferritin. Deep gray matter nuclei have the highest concentrations of non-heme iron in the brain. Many of these nuclei naturally accrue iron with age,[16] but abnormally high levels have been implicated in many neurodegenerative diseases, including MS.[17]

Whether iron accumulation is a neurodegenerative factor or a benign by-product of the disease, it may serve as a biomarker of disease severity and state.[15] Quantitative imaging methods that are sensitive to non-heme iron could identify and exploit this potential biomarker.

Numerous MRI studies of MS have been performed at 1.5 T, and more recently, at 3.0 T.[18] Sensitivity to iron increases with field strength,[19,20] and a near-linear increase in signal-to-noise ratio with field strength enables detailed visualization of iron distribution. Very high field (VHF) systems, defined loosely as those exceeding 3.0 T, are promising tools for visualization of brain iron and have been employed for improved lesion detection, morphological analysis, and for vascular imaging.

Quantitative methods at VHF are particularly desirable for measurement of iron content. Currently, no absolute quantitative measure of iron is possible using MRI; however, numerous methods are highly sensitive to its effects. Notably, transverse relaxometry measures are sensitive to *intra-voxel phase variation* while susceptibility phase imaging relates to the *average intra-voxel phase shift* within iron-rich structures. Historically, these methods have rarely been employed together at VHF due to methodological limitations.

The spin echo transverse relaxation rate (R_2) has an iron relaxivity that increases linearly with field strength[19] and may prove sufficiently sensitive and specific to become a reliable measure of brain iron at VHF. In addition, R_2 mapping is insensitive to macroscopic background field gradients, including those surrounding large vasculature. Historically, its use on VHF systems has been extremely limited owing to excessive radiofrequency (RF) field heterogeneity and high RF power deposition required to achieve a train of spin echoes. A new analysis method that corrects for stimulated echoes enables accurate R_2 mapping in heterogeneous RF fields,[21] although RF power deposition restrictions still preclude efficient volume coverage.

The gradient echo transverse relaxation rate (R_2^*) is very sensitive to iron but is influenced by magnetic field gradients surrounding air/tissue boundaries, large draining veins, and tissue microvasculature. These deleterious effects are exacerbated at VHF. Recently, several works have described correction methods to rescale the signal intensity in regions of strong background field gradients, enabling reduced artifacts in 2D multislice imaging[22] and transverse relaxometry,[23] and 3D transverse relaxometry.[24] Both R_2 and R_2^* relaxation measures are confounded by changes in tissue water and macro-molecular content – rates decrease with increased cellular water concentration – thus clouding interpretation of these parameters. Nevertheless, both have been applied to study white matter and deep gray matter in MS, but only at clinical field strengths.[25-27]

Phase susceptibility imaging[28,29] is sensitive to local field shifts caused by the magnetic susceptibility of tissues. Iron is paramagnetic and tends to enhance the local field within iron-rich tissues. These shifts can be visualized and quantified on processed (typically high-pass filtered) phase images, obtained from a standard gradient echo acquisition. Unfortunately, the method is prone to artifacts due to the filtering process and inherent susceptibility effects. Despite limitations, phase imaging can be very sensitive to iron and has been used to visualize venous vasculature,[29] characterize lesions,[30,31] and to quantify the local field shift (LFS) in sub-cortical gray matter of patients with relapsing–remitting MS (RRMS).[32]

The use of multiple, complementary iron-sensitive measures can provide a more definite conclusion as to the presence of iron, given the limitations of each method, such as artifacts in LFS and water content in transverse relaxometry. Previously, technical challenges have precluded simultaneous application of these quantitative MRI methods to a patient population at very high field. This study uses novel VHF optimized R_2[21] and R_2^*[24] relaxometry methods and susceptibility phase imaging at 4.7 T to perform, for the first time, a multi-modal study of iron accumulation in sub-cortical gray matter of patients with early-stage RRMS.

Materials and methods

For this study, 22 patients with RRMS and 22 age- and gender-matched controls were recruited (Table 1). Patients were enrolled consecutively based on presentation to the clinic using the following inclusion criteria: a diagnosis of RRMS according to the McDonald criteria[33] and an Expanded Disability Status Scale (EDSS) score less than or equal to 6.0. Exclusion criteria for all subjects were: non-MS-related neurological disease, significant medical illness that could influence MRI findings, and MRI contraindications. All subjects provided informed consent, in compliance with institutional regulations, prior to participation.

Imaging was performed on a Varian Unity Inova 4.7 T MRI with a maximum gradient strength of 60 mT/m and slew rate of 120 T/m/s. Images were collected with a

Table 1. Subject demographics.

	Patients (n = 22)	Controls (n = 22)
Gender, M/F	5/17	5/17
Age, Mean ± SD (years)	33.4 ± 7.4	33.4 ± 6.9
Disease duration, Mean ± SD (years)	3.4 ± 2.8	—
EDSS, Mean ± SD (years)	2.5 ± 1.4	—

EDSS, Expanded Disability Status Scale

Table 2. Acquisition parameters for quantitative imaging.

Parameter	R_2	R_2^*	LFS
Voxel volume (mm^3)	5.00	2.00	0.75
In-plane resolution (mm^2)	1.00 × 1.25	1.00 × 1.00	0.50 × 0.75
Slice thickness (mm)	4.00	2.00	2.00
Number of slices	2	90	50
Repetition time (ms)	3500	44	1540
First echo time (ms)	10.0	2.93	15.0
Echo spacing (ms)	10.0	4.10	—
Echo train length	20	10	—
Tip angle (deg)	90x–180y–180y…	10	65
Acquisition time (min)	4.5	9.4	6.6

LFS, local field shift

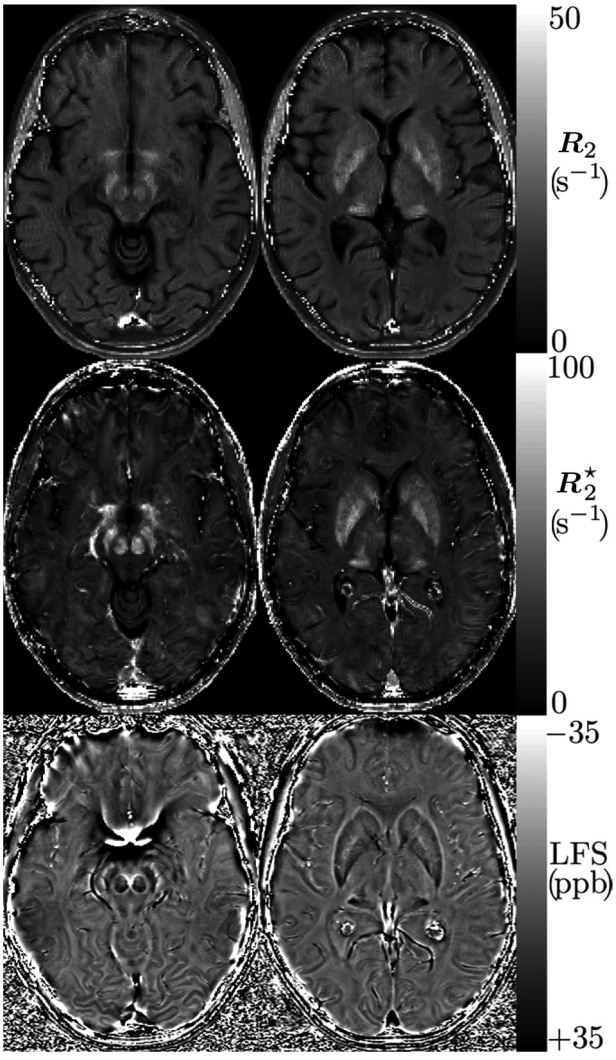

Figure 1. Quantitative magnetic resonance images of a 34-year-old patient with multiple sclerosis at 4.7T.
R_2 maps (top row) are scaled from 0 to 50 s^{-1}, R_2^* maps (middle row) from 0 to 100 s^{-1}, susceptibility phase (bottom row) from -0.2π to 0.2π (equivalent to local field shift from 35 to -35 ppb). Strong contrast is observed between basal ganglia structures and surrounding tissue for all three methods.

4-element receive array paired with a birdcage coil for transmit. Three quantitative imaging sequences were acquired in the axial plane: a 2D multislice multiecho spin echo for R_2, a 3D multiecho gradient echo for R_2^*, and a 2D multislice flow-compensated gradient echo for LFS (Table 2, Figure 1). The R_2^* and LFS volumes encompassed all of the deep gray matter structures, while the R_2 protocol was limited to two slices to maintain RF power deposition within safety limits. One slice was placed through the globus pallidus, caudate nucleus, putamen, internal capsule, and thalamus; the other through the substantia nigra and red nucleus.

Quantitative R_2 maps were processed using the stimulated echo compensating fit to account for the heterogeneous RF transmit field;[21] R_2^* maps employed 3D susceptibility compensation to reduce the deleterious effects of static field gradients surrounding air–tissue interfaces.[24] Susceptibility phase images (Φ) were obtained by dividing the original complex gradient echo image by a low-pass filtered version, smoothed with a 2D Gaussian frequency kernel that extended over one-eighth of the k-space matrix, then measuring the resulting phase angle. Phase angles were converted to LFS,[32] measured in parts-per-billion (ppb), via

$$\mathrm{LFS} = \frac{-\Phi}{2\pi\gamma \mathrm{B}_0 \mathrm{TE}}$$

to facilitate comparison between field strengths (B_0) and echo times (TE).

Using the resolution- and coverage-limiting R_2 images, bilateral regions-of-interest (ROIs) (Figure 2) were drawn around the globus pallidus, putamen, head of the caudate nucleus, substantia nigra, and the red nucleus. The thalamus was sub-divided into the pulvinar nucleus and the remainder of the thalamus. This thalamic sub-division was done for two reasons: first, reliable contrast between the pulvinar and the remainder of the thalamus was observed on all quantitative images, unlike other sub-thalamic nuclei, which appeared anatomically indistinct. Second, pulvinar hypointensity on susceptibility phase images has

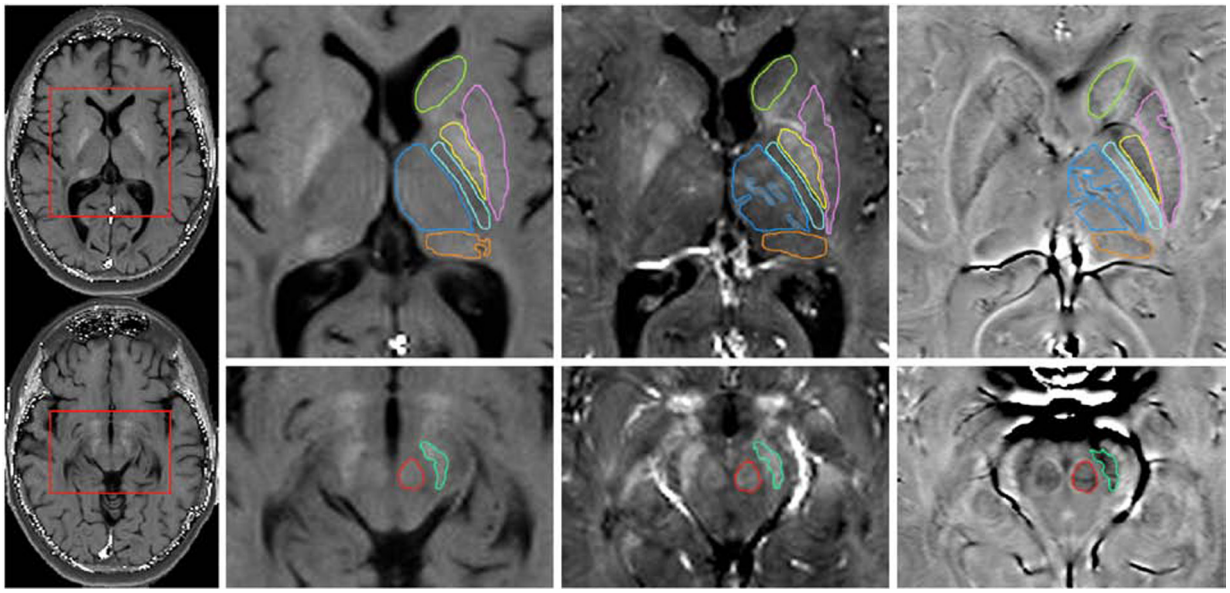

Figure 2. Typical ROI placement on quantitative images of a 24-year-old patient with relapsing–remitting multiple sclerosis.
Full field-of-view R_2 maps are shown in the far left column. Regions of interest (ROIs) covering the caudate nucleus (light green), putamen (pink), globus pallidus (yellow), thalamus (dark blue), pulvinar (orange), substantia nigra (dark green), red nucleus (red), and internal capsule (light blue) are overlaid on the cropped R_2 maps (center left column), R_2^* maps (center right column), and the susceptibility phase images (far right column). Images are scaled as in Figure 1. Unilateral ROIs are shown for display purposes; bilateral ROIs were analyzed. Slight ROI modification was required between series to account for subject motion, vasculature, and background field gradients.

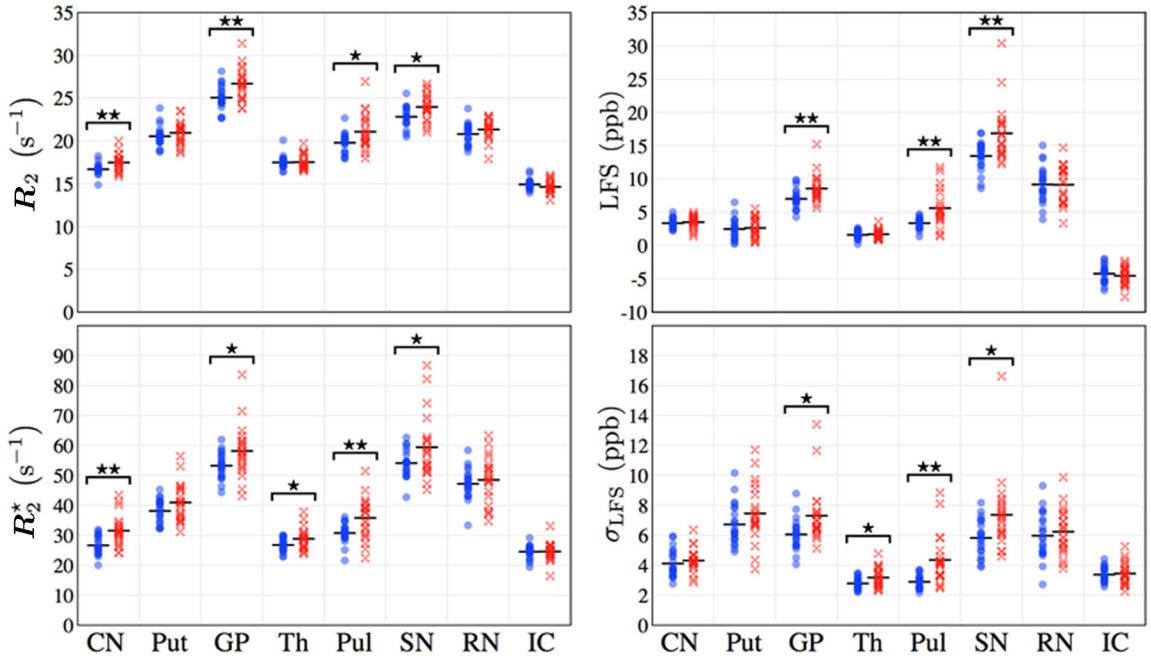

Figure 3. Quantitative magnetic resonance imaging parameters are shown in healthy controls (circles) and in patients with multiple sclerosis (MS) (crosses). Starred comparisons indicate $p < 0.05$; double starred, $p < 0.006$. The pulvinar, globus pallidus, and substantia nigra show significant group differences on all measures; most other deep gray matter structures in patients with MS show significant differences from control subjects on one or more measures. (CN, caudate nucleus; Put, putamen; GP, globus pallidus; Th, thalamus; Pul, pulvinar; SN, substantia nigra; RN, red nucleus; IC, internal capsule).

Table 3. Percent change and effect size for quantitative MRI parameters in patients with MS relative to controls. Bold-faced values are significant at the $p < 0.05$ level; underlined values at $p < 0.006$. Italicized values are not significant.

Region	R_2		R_2^*		LFS		σ_{LFS}	
	PC	ES	PC	ES	PC	ES	PC	ES
CN	**4.59**	**0.95**	**16.89**	**1.21**	*4.60*	*0.19*	*4.92*	*0.25*
Put	*1.99*	*0.33*	*7.14*	*0.55*	*6.35*	*0.11*	*10.25*	*0.45*
GP	**6.37**	**1.02**	**8.78**	**0.76**	**19.96**	**0.90**	**18.66**	**0.86**
Th	*0.15*	*0.03*	**7.47**	**0.73**	*5.64*	*0.14*	**13.10**	**0.77**
Pul	**6.26**	**0.81**	**15.14**	**1.00**	**50.08**	**1.26**	**40.24**	**1.42**
SN	**4.89**	**0.85**	**9.31**	**0.70**	**22.44**	**1.07**	**23.37**	**0.84**
RN	*2.52*	*0.43*	*2.71*	*0.20*	*–0.43*	*–0.01*	*4.23*	*0.17*
IC	*–2.00*	*–0.45*	*0.23*	*0.02*	*7.37*	*–0.24*	*1.87*	*0.10*

LFS, local field shift; PC, Percent Change; ES, Effect Size; CN, Caudate Nucleus; Put, Putamen; GP, Globus Pallidus; Th, Thalamus; Pul, Pulvinar; SN, Substantia Nigra; RN, Red Nucleus; IC, Internal Capsule

been reported in a patient with MS.[30] The only white matter region analyzed was the internal capsule. If required, ROIs were modified on R_2^* and LFS maps to compensate for inter-scan motion, to exclude confounding vasculature, to exclude lesions in MS patients, and to avoid the effects of uncorrected background field gradients. This slight ROI modification was required to capitalize on the strengths of each method while avoiding its weaknesses. LFS is not referenced to neighboring tissue, such as a ventricle or normal-appearing white matter. Analysis was non-blinded since subjects could be readily categorized from the MR images due to the presence of white matter lesions. All ROIs were drawn by the same individual (RML) and were obtained in a systematic manner for all subjects.

Parameter values were averaged within ROIs and between hemispheres. The standard deviation of the LFS (σ_{LFS}) within each ROI was also measured. This provides an alternate measure for susceptibility phase that is complementary to averaging and helps negate the deleterious effects of high-pass filtering and of dipole field projections. Parameters were compared with those from healthy controls using a two-tailed Student's *t*-test. The percent change between the inter-patient and inter-control mean was calculated for each brain region and quantitative measure. The effect size, defined as the difference of means divided by the average of standard deviations, is also reported. Pearson product-moment correlation coefficients were calculated between MRI parameters and both the EDSS and disease duration, the latter defined as the duration of time between the index relapse and the MRI exam. Group differences and correlations at the $p<0.05$ significance level are noted; differences satisfying $p<0.006$ – a level obtained via Bonferroni correction for eight independent ROIs – are considered highly significant.

Results

Group averaged quantitative MRI measures were higher in patients with MS than in controls in all sub-cortical gray matter regions investigated (Figure 3, Table 3), with the exception of LFS in the red nucleus. While these group differences were not statistically significant in all regions – the putamen and red nucleus lacked significance in all measures – all other gray matter regions had significance below $p=0.05$ in two or more measures. The globus pallidus, pulvinar, and substantia nigra of patients with MS were abnormal in all measures, often at $p<0.006$. The pulvinar demonstrated the largest percent change and effect size in phase measurements and is comparable with the largest percent change and effect size in the relaxation measures; it was the most abnormal region we measured. In contrast to the pulvinar, the remainder of the thalamus had only mildly significant changes in R_2^* and σ_{LFS}. The caudate nucleus appeared abnormal in relaxation measures, but lacked significance in phase measures. No significant abnormality was observed in the internal capsule.

A total of four regions showed abnormalities with $p<0.006$ (Figure 3); however, their identification required the use of multiple quantitative measures. The caudate was identified by relaxometry measures, the globus pallidus by R_2 and LFS, the pulvinar by R_2^*, LFS, and σ_{LFS}, and the substantia nigra by LFS. R_2^* provided larger percent changes than did R_2 in all regions (Table 3); however, larger standard deviations in R_2^* than in R_2 resulted in comparable effect sizes. Both relaxometry methods identified two regions with high significance. The LFS and σ_{LFS} had the largest percent change and effect size, respectively, indicating the potential sensitivity of phase methods for iron detection. These metrics also had marked variation in these parameters. The discrepancy in percent change and effect size between LFS and σ_{LFS}, particularly in large structures such as the putamen and thalamus, (Figure 3, Table 3) suggest that information contained in phase images is not being captured effectively.

Six significant correlations with EDSS, two of which were significant below $p=0.006$, were observed in three different brain regions (Figure 4). R_2^* correlated strongly ($R\approx0.62$) in the thalamus and pulvinar nucleus. Moderate

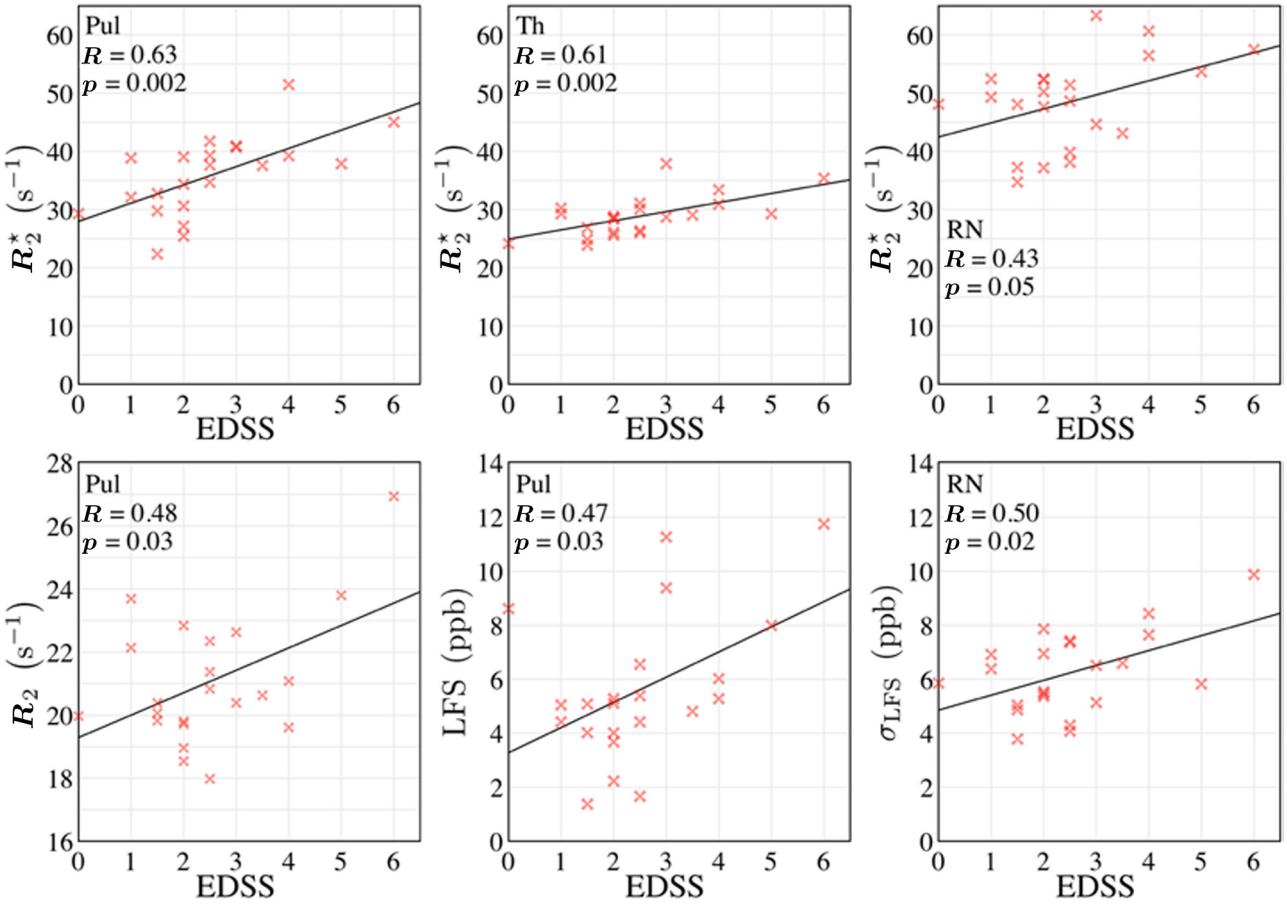

Figure 4. Significant correlations between quantitative magnetic resonance imaging parameters and Expanded Disability Status Scale (EDSS). Strong correlations were observed in the pulvinar nucleus when measured with R_2^*. This finding is supported with moderate correlations when measured with R_2 and local field shift. The red nucleus and thalamus were also found to correlate with EDSS. R_2^* mapping identified all three of these regions; the other metrics proved less sensitive than, but remained consistent with, R_2^*. (Th, thalamus; Pul, pulvinar; RN, red nucleus).

correlations ($R \approx 0.47$) in the pulvinar were also observed with R_2 and LFS. Moderate correlations ($R \approx 0.46$) with EDSS were also observed in the red nucleus with R_2^* and σ_{LFS}. Consistency is observed between imaging sequences: both relaxometry metrics and the LFS indicate pulvinar abnormalities that worsen with increasing EDSS. Furthermore, the red nucleus is implicated with two independent measures, albeit both near the $p = 0.05$ significance threshold. R_2^* was the only modality to identify all three regions in which correlations were observed, although the other metrics reinforced these observations.

No significant correlations were observed between MRI parameters and disease duration in any brain region.

Discussion

Multiple deep gray matter regions had abnormal MRI parameters in patients with early-stage RRMS. The most affected regions are the pulvinar, globus pallidus, and substantia nigra. The caudate nucleus, and the thalamus were also observed to be abnormal relative to healthy controls; these changes were only detected with two of the four imaging metrics. Even for gray matter regions in which differences did not reach statistical significance, group averaged relaxation rates and field shifts were elevated in the MS group relative to controls. No significant abnormalities were observed in the internal capsule. Overall, widespread abnormalities were observed in the sub-cortical gray matter of patients with early-stage RRMS.

We observed a strong correlation with EDSS in the pulvinar nucleus, and moderate correlations were detected in the thalamus and red nucleus. The functional properties of these affected nuclei are complex and associate broadly with multiple systems in the central nervous system. Although pulvinar function is poorly understood due to complex and diffuse cortical projections, it is known to have an important role as a visual relay.[34] The red nucleus has afferent connections with the motor cortex and cerebellum and efferent connections in the rubrospinal tract, which modulates flexor muscle tone. Thalamic abnormalities may

be broadly attributed to numerous functional systems, such as sensory deficits and motor control. All of these systems register on the EDSS scale.

A recent work found mildly significant hypointensity on T_2-weighted images of patients with clinically isolated syndromes.[5] This work reports slight hypointensity throughout the basal ganglia, albeit significant only in the left caudate nucleus. Our transverse relaxometry measurements in the present RRMS cohort are consistent with their findings. The substantia nigra has appeared normal on T_2 weighting scans at 1.5 T.[4] We observed a potential increase in R_2 and R_2^* and an enhancement in susceptibility phase change in this region. We attribute our observations to increased sensitivity at VHF relative to clinical field strengths.

Lack of correlation between MRI parameters and disease duration may be due to the small variance in our MS group: the average disease duration was 3.4 ± 2.8 years and ranged from 0.3–11.6 years. The regions investigated here do not appear to change over this span of disease duration at a rate that can be detected with our methods. The lack of correlation in this population with early-stage disease is not surprising, since it is known that there is variability in time from onset of MS disease pathology to the time of recognized index relapse.

Patient populations with a larger disease duration variance may elicit correlations, as recently reported at 7 T using susceptibility phase imaging.[32] Our LFS results confirm Hammond et al.'s report of abnormal LFS in the basal ganglia. In both studies, the globus pallidus shows a large increase in the local field while the thalamus shows a small field increase. The 7 T report also observed LFS changes in the caudate and putamen, neither of which differed in phase measurements reported here. However, the 7 T study investigated patients with a much longer disease duration (12.0 ± 7.6 years) than the current work (3.4 ± 2.8 years) and reported correlations with disease duration in these two (and *only* these two) regions. The *lack* of LFS abnormality in the striatum observed in our work is consistent with the 7 T report. The Hammond study did not observe correlations between LFS and EDSS; our highly sensitive relaxometry methods and thalamic sub-division show correlations for the first time.

We attribute elevated MRI parameters in patients relative to controls to iron accumulation, which is reported to occur in the sub-cortical gray matter of patients with MS,[3,25] and to which these quantitative measures are known to be sensitive.[19,28,35] While relaxation rates can be altered by proton mobility, this is an unlikely explanation for the observed increases in relaxation rates. Loss of neuronal membrane integrity, myelin decomposition, and cellular edema will *decrease* R_2[36] and R_2^*. Furthermore, evidence suggests the mean diffusivity in the basal ganglia is not significantly altered in RRMS and secondary-progressive MS,[37,38] suggesting that the relaxation changes we observe are not due to water content and tissue integrity confounds. Tissue iron remains the most likely cause of abnormal transverse relaxation rates and image phase in deep gray matter.

Unfortunately, the MRI measures provide little insight into the exact form or origin of the iron. Susceptibility phase imaging detects the bulk field shift within a paramagnetic region, while relaxometry measures are sensitive to microscopic magnetic field fluctuations surrounding paramagnetic particles. The paramagnetic material is likely non-heme iron in the form of ferritin, since heme iron was recently excluded as a dominant contrast mechanism within tissues on susceptibility images.[39] As such, our finding of increased relaxation rates and LFS implies an increase in ferritin-bound iron. This observation correlates with pathological findings in MS in which ferritin iron has been reported.[2]

We believe a combined approach including a transverse relaxometry measure (R_2^* proved particularly useful in this work) and susceptibility phase imaging is promising for VHF MRI evaluation of MS pathogenesis. Firstly, the sensitivity of each method is likely to depend on the distribution of tissue iron, potentially causing a differential enhancement between the various methods. Secondly, the processing required to extract LFS attenuates contrast in large homogeneous structures. In this study, LFS in the putamen, thalamus, and caudate may be artificially low. In these structures, metrics such as σ_{LFS} show greater percent change and effect size and may be more representative of tissue properties than the average LFS. Ultimately, the use of multiple, complementary iron-sensitive measures and processing methods can provide a more definite conclusion as to the presence of iron, given the limitations of each method, such as artifacts in LFS, and water content in transverse relaxometry.

In conclusion, very high-field MRI with multiple quantitative measures revealed widespread abnormalities in the deep gray matter of patients with early-stage RRMS. The most abnormal region was the pulvinar nucleus, which showed increased transverse relaxation rates and LFS relative to control subjects and displayed strong correlations between these MRI measures and EDSS. R_2^* mapping proved to be the most reliable metric for detecting differences between patients with MS and controls, and also gave the strongest correlations with EDSS; however, the use of multiple quantitative protocols was required to discern all affected regions, and was beneficial in confirming correlations with neurological deficits.

Acknowledgements

The authors wish to thank Dr Edward Johnson (Division of Anatomical Pathology, University of Alberta) for helpful discussion.

Funding

This work was supported by the Canadian Institutes of Health Research [grant number MOP-102582]; the Natural Sciences and the Engineering Research Council of Canada [grant number 32773]; the Multiple Sclerosis Society of Canada; and the University of Alberta Hospital Foundation. Salary support by Alberta Innovates – Health Solutions (RML).

Conflict of interest statement

The authors declare that there are no conflicts of interest.

References

1. Craelius W, Migdal MW, Luessenhop CP, Sugar A and Mihalakis I. Iron deposits surrounding multiple sclerosis plaques. *Arch Pathol Lab Med* 1982; 106: 397–399.
2. LeVine SM. Iron deposits in multiple sclerosis and Alzheimer's disease brains. *Brain Res* 1997; 760: 298–303.
3. Drayer B, Burger P, Hurwitz B, Dawson D and Cain J. Reduced signal intensity on MR images of thalamus and putamen in multiple sclerosis: increased iron content? *Am J Roentgenol* 1987; 149: 357–363.
4. Bakshi R, Benedict RHB, Bermel RA, et al. T2 hypointensity in the deep gray matter of patients with multiple sclerosis: a quantitative magnetic resonance imaging study. *Arch Neurol* 2002; 59: 62–68.
5. Ceccarelli A, Rocca MA, Neema M, et al. Deep gray matter T2 hypointensity is present in patients with clinically isolated syndromes suggestive of multiple sclerosis. *Mult Scler* 2010; 16: 39–44.
6. Tjoa CW, Benedict RHB, Weinstock-Guttman B, Fabiano AJ and Bakshi R. MRI T2 hypointensity of the dentate nucleus is related to ambulatory impairment in multiple sclerosis. *J Neurol Sci* 2005; 234: 17–24.
7. Ge Y, Jensen JH, Lu H, et al. Quantitative assessment of iron accumulation in the deep gray matter of multiple sclerosis by magnetic field correlation imaging. *AJNR Am J Neuroradiol* 2007; 28: 1639–1644.
8. Neema M, Arora A, Healy BC, et al. Deep gray matter involvement on brain mri scans is associated with clinical progression in multiple sclerosis. *J Neuroimag* 2009; 19: 3–8.
9. Brass SD, Benedict RH, Weinstock-Guttman B, Munschauer F and Bakshi R. Cognitive impairment is associated with subcortical magnetic resonance imaging grey matter T2 hypointensity in multiple sclerosis. *Mult Scler* 2006; 12: 437–444.
10. Houtchens MK, Benedict RH, Killiany R, et al. Thalamic atrophy and cognition in multiple sclerosis. *Neurology* 2007; 69: 1213–1223.
11. Miki Y, Grossman RI, Udupa JK, et al. Relapsing-remitting multiple sclerosis: longitudinal analysis of MR images – lack of correlation between changes in T2 lesion volume and clinical findings. *Radiology* 1999; 213: 395–399.
12. Galaris D and Pantopoulos K. Oxidative stress and iron homeostasis: mechanistic and health aspects. *Crit Rev Clin Lab Sci* 2008; 45: 1–23.
13. Kell DB. Iron behaving badly: inappropriate iron chelation as a major contributor to the aetiology of vascular and other progressive inflammatory and degenerative diseases. *BMC Med Genomics* 2009; 2: 2.
14. Koppenol WH. The Haber-Weiss cycle – 70 years later. *Redox Rep* 2001; 6: 229–234.
15. Schenck JF and Zimmerman EA. High-field magnetic resonance imaging of brain iron: birth of a biomarker? *NMR Biomed* 2004; 17: 433–445.
16. Hallgren B and Sourander P. The effect of age on the non-haemin iron in the human brain. *J Neurochem* 1958; 3: 41–51.
17. Pinero DJ and Connor JR. Iron in the brain: an important contributor in normal and diseased states. *Neuroscientist* 2000; 6: 435–453.
18. Ropele S, de Graaf W, Khalil M, et al. MRI assessment of iron deposition in multiple sclerosis. *J Magn Reson Imaging* 2011; 34: 13–21.
19. Gelman N, Gorell JM, Barker PB, et al. MR imaging of human brain at 3.0 T: preliminary report on transverse relaxation rates and relation to estimated iron content. *Radiology* 1999; 210: 759–767.
20. Yao B, Li T-Q, Gelderen Pv, Shmueli K, de Zwart JA and Duyn JH. Susceptibility contrast in high field MRI of human brain as a function of tissue iron content. *Neuroimage* 2009; 44: 1259–1266.
21. Lebel RM and Wilman AH. Transverse relaxometry with stimulated echo compensation. *Magn Reson Med* 2010; 64: 1005–1014.
22. Volz S, Hattingen E, Preibisch C, Gasser T and Deichmann R. Reduction of susceptibility-induced signal losses in multi-gradient-echo images: application to improved visualization of the subthalamic nucleus. *Neuroimage* 2009; 45: 1135–1143.
23. Baudrexel S, Volz S, Preibisch C, et al. Rapid single-scan T2*-mapping using exponential excitation pulses and image-based correction for linear background gradients. *Magn Reson Med* 2009; 62: 263–268.
24. Lebel RM and Wilman AH. Field-corrected 3D multiecho gradient echo: simultaneous extraction of quantitative R2*, T2* weighting, SWI, and venography. *Joint Annual Meeting of the ISMRM-ESMRMB*. Stockholm, Sweden 2010, p. 5002.
25. Khalil M, Enzinger C, Langkammer C, et al. Quantitative assessment of brain iron by R2* relaxometry in patients with clinically isolated syndrome and relapsing–remitting multiple sclerosis. *Mult Scler* 2009; 15: 1048–1054.
26. Neema M, Goldberg-Zimring D, Guss ZD, et al. 3 T MRI relaxometry detects T2 prolongation in the cerebral normal-appearing white matter in multiple sclerosis. *Neuroimage* 2009; 46: 633–641.
27. Burgetova A, Seidl Z, Krasensky J, Horakova D and Vaneckova M. Multiple sclerosis and the accumulation of iron in the basal ganglia: quantitative assessment of brain iron using MRI T2 relaxometry. *Eur Neurol* 2010; 63: 136–143.
28. Ogg RJ, Langston JW, Haacke EM, Steen RG and Taylor JS. The correlation between phase shifts in gradient-echo MR images and regional brain iron concentration. *Magn Reson Imaging* 1999; 17: 1141–1148.
29. Haacke EM, Xu Y, Cheng YC and Reichenbach JR. Susceptibility weighted imaging (SWI). *Magn Reson Med* 2004; 52: 612–618.
30. Haacke EM, Makki M, Ge Y, et al. Characterizing iron deposition in multiple sclerosis lesions using susceptibility weighted imaging. *J Magn Reson Imaging* 2009; 29: 537–544.

31. Eissa A, Lebel RM, Korzan JR, et al. Detecting lesions in multiple sclerosis at 4.7 Tesla using phase susceptibility-weighting and T2-weighting. *J Magn Reson Imaging* 2009; 30: 737–742.
32. Hammond KE, Metcalf M, Carvajal L, et al. Quantitative in vivo magnetic resonance imaging of multiple sclerosis at 7 Tesla with sensitivity to iron. *Ann Neurol* 2008; 64: 707–713.
33. Polman CH, Reingold SC, Edan G, et al. Diagnostic criteria for multiple sclerosis: 2005 revisions to the "McDonald Criteria". *Ann Neurol* 2005; 58: 840–846.
34. Leh SE, Chakravarty MM and Ptito A. The connectivity of the human pulvinar: a diffusion tensor imaging tractography study. *J Vision* 2007; 7: 224.
35. Mitsumori F, Watanabe H and Takaya N. Estimation of brain iron concentration in vivo using a linear relationship between regional iron and apparent transverse relaxation rate of the tissue water at 4.7T. *Magn Reson Med* 2009; 62: 1326–1330.
36. Laule C, Vavasour IM, Moore GRW, et al. Water content and myelin water fraction in multiple sclerosis. *J Neurol* 2004; 251: 284–293.
37. Ciccarelli O, Werring DJ, Wheeler-Kingshott CAM, et al. Investigation of MS normal-appearing brain using diffusion tensor MRI with clinical correlations. *Neurology* 2001; 56: 926–933.
38. Filippi M, Bozzali M and Comi G. Magnetization transfer and diffusion tensor MR imaging of basal ganglia from patients with multiple sclerosis. *J Neurol Sci* 2001; 183: 69–72.
39. Marques JP, Maddage R, Mlynarik V and Gruetter R. On the origin of the MR image phase contrast: an in vivo MR microscopy study of the rat brain at 14.1 T. *Neuroimage* 2009; 46: 345–352.